The Sedimentary Context of El Kherba Early Pleistocene Oldowan Site, Algeria: Sediment and Soil Micromorphology Studies

Salah Abdessadok, Mohamed Sahnouni, Zoheir Harichane, Nacim Mazouni, Razika Chelli Cheheb, Yasmine Mouhoubi, Saloua Chibane, Alfredo Pérez-González

frontiers | Frontiers in Earth Science

ORIGINAL RESEARCH
published: 20 June 2022
doi: 10.3389/feart.2022.893473

The Sedimentary Context of El Kherba Early Pleistocene Oldowan Site, Algeria: Sediment and Soil Micromorphology Studies

Salah Abdessadok[1,2], *Mohamed Sahnouni*[3,2,4]*, *Zoheir Harichane*[5,2], *Nacim Mazouni*[2,6], *Razika Chelli Cheheb*[2], *Yasmine Mouhoubi*[2], *Saloua Chibane*[2] *and Alfredo Pérez-González*[7]

[1]Histoire Naturelle de l'Homme Préhistorique (HNHP), UMR7194, Muséum national d'histoire naturelle, CNRS, Université Perpignan via Domitia, Alliance Sorbonne Université, Paris, France, [2]Centre National de Recherches Préhistoriques, Anthropologiques et Historiques (CNRPAH), Sidi M'Hamed, Algeria, [3]Centro Nacional de Investigación sobre la Evolución Humana (CENIEH), Burgos, Spain, [4]Anthropology Department, Stone Age Institute, Indiana University, Bloomington, IN, United States, [5]Musée National du Bardo, Sidi M'Hamed, Algeria, [6]Departament d'Historia i Historia de Art, Universitat Rovira i Virgili, Tarragona, Spain, [7]IDEA (Instituto de Evolución en África), University of Alcalá de Henares, Madrid, Spain

OPEN ACCESS

Edited by:
Marie-Hélène Moncel, Director of Research CNRS-MNHN, France

Reviewed by:
Michael Chazan, University of Toronto, Canada
Mathieu Rué, Paléotime, France

***Correspondence:**
Mohamed Sahnouni
mohamed.sahnouni@cenieh.es

Specialty section:
This article was submitted to Quaternary Science, Geomorphology and Paleoenvironment, a section of the journal Frontiers in Earth Science

Received: *10 March 2022*
Accepted: *29 April 2022*
Published: *20 June 2022*

Citation:
Abdessadok S, Sahnouni M, Harichane Z, Mazouni N, Chelli Cheheb R, Mouhoubi Y, Chibane S and Pérez-González A (2022) The Sedimentary Context of El Kherba Early Pleistocene Oldowan Site, Algeria: Sediment and Soil Micromorphology Studies. Front. Earth Sci. 10:893473. doi: 10.3389/feart.2022.893473

A comprehensive investigation is conducted on the archeological sediments from the Early Pleistocene site of El Kherba (Algeria), involving sediment and soil micromorphology analyses. El Kherba yielded Oldowan stone tools associated with animal fossils from three archeological levels. The studies aim at assessing the sedimentary processes that acted in the burial of the archeological remains and at identifying microfacies in order to gain high-resolution paleoenvironmental information pertaining to early hominin behavioral activities at the site 1.8 million years ago. The data indicate that the archeological assemblages accumulated in sediments with fine-grained particles, primarily silt and clay of massive structure, in a floodplain landscape in a temperate climate in the lower part of the stratigraphy and a gradual change from humid to arid environment in the upper part. These results are also supported by taphonomic and isotope studies carried out previously on the site.

Keywords: grain size, micromorphology, El Kherba, Oldowan, Early Pleistocene, Algeria, Lower Paleolithic

1 INTRODUCTION

Appraising site formation processes is nowadays an essential component in Paleolithic studies. It seeks to decipher the nature of the agencies, geological or behavioral, which were primarily involved in the accumulation of fossil bones and stone artifacts in early Paleolithic sites. This enquiry is commonly approached by 1) assessing the taphonomic grade of fossil bones (e.g., Shipman, 1981; Lyman, 1994) and 2) identifying agents responsible for stone artifact concentrations (e.g., Schick, 1986). While bone taphonomic conditions and artifact concentration patterns are important criteria, the sediments encasing the archeological remains are equally crucial for reconstructing site formation processes (e.g., Hassan, 1978). They represent a line of evidence of major interest for contextualizing Paleolithic archeological assemblages. Moreover, the sediments are considered "artifacts" as they are tightly part of the archeological record along with other behavioral objects (Goldberg and Berna, 2010). They provide valuable information not only on the depositional dynamics by which artifacts were incorporated into the sedimentary matrix but also on the paleoenvironmental conditions prevailing during early hominin behavioral activities.

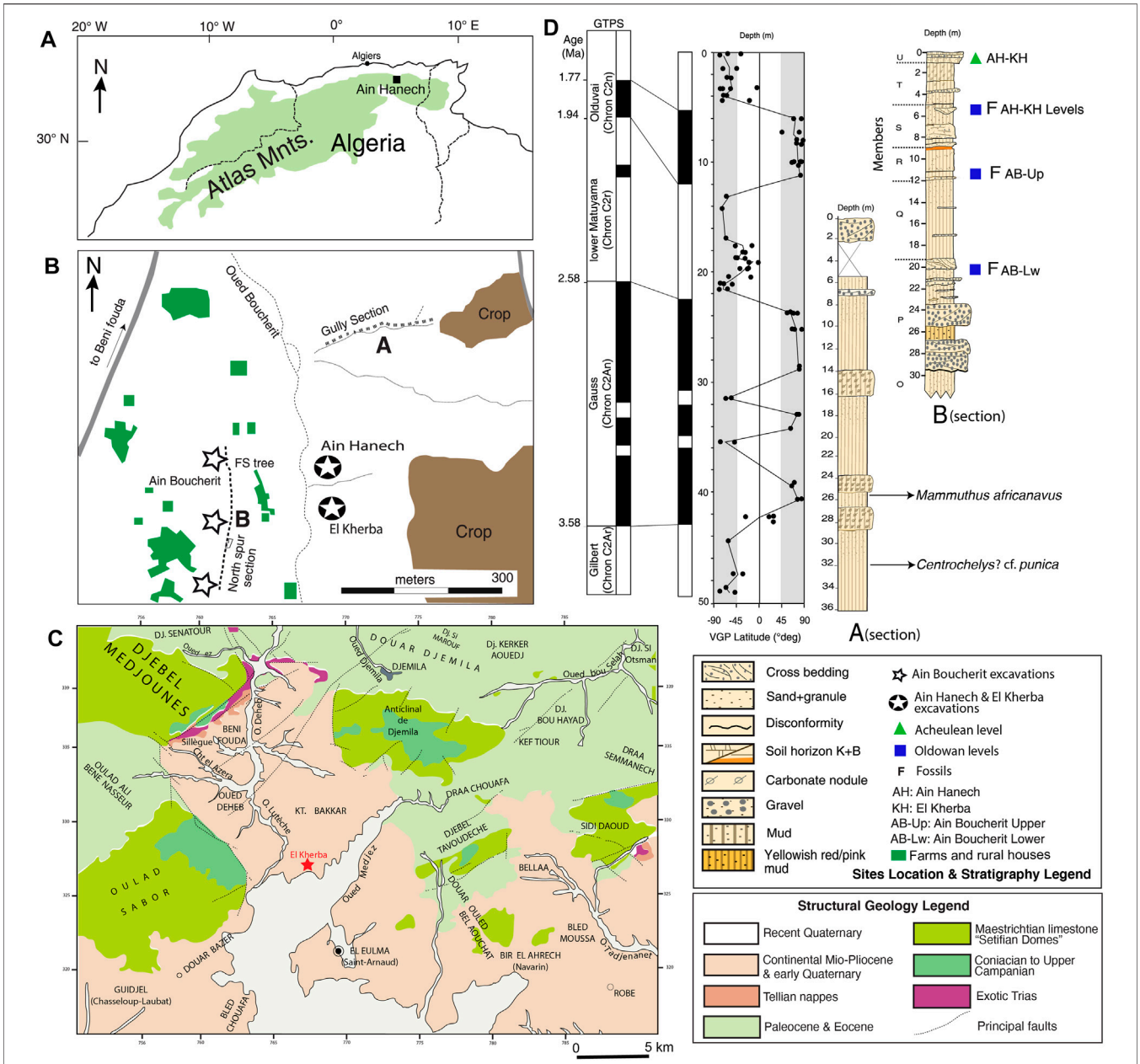

FIGURE 1 | Geography and geology of El Kherba, including **(A)** geographic situation of the Ain Hanech research area within Algeria, **(B)** situation of the El Kherba Oldowan site within the Ain Hanech research area, **(C)** El Kherba regional geological context (redrawn after El Eulma geological map, 1/50 000, 1977), and **(D)** stratigraphic and magnetostratigraphic position of El Kherba deposit within the Ain Hanech formation (modified after Sahnouni, 1998).

Comprehensive examination, usually employed in Paleolithic archeology to assess the sedimentary context of archeological assemblages, comprises chiefly three lines of evidence: stratigraphic description, grain size characteristics, and soil micromorphology. The stratigraphic evidence provides a gross depiction of the sedimentary context of the archeological remains, e.g., fine-grained versus coarse-grained sediments. The size of sedimentary particles is indicative of flow velocity (Hassan, 1978). For instance, fine-grained sediments settle from suspension at a lower velocity regime, such as particles deposited in lakes and flood basins. On the contrary, coarser grains such as sands and gravels are deposited at river channels with a high velocity regime. Soil micromorphology provides high-resolution data that "can discriminate the sedimentary signatures diagnostic of human-related activities from natural phenomena" (Courty, 1992). Furthermore, it offers detailed paleoenvironmental information that can help reconstruct early hominin behaviors and their use of the landscapes (Mallol, 2006; Mallol et al., 2011).

This paper presents detailed sedimentological and micromorphological studies of the fluvial sediments containing

the Oldowan assemblages of the Early Pleistocene site of El Kherba in northern Algeria. The studies aim at appraising the processes that acted in the accumulation of the archeological remains at the site and at identifying microfacies in order to acquire high-resolution paleoenvironmental data that took place at El Kherba 1.8 million years ago (Ma). After conducting analyses on stone artifact concentrations (Sahnouni and de Heinzelin, 1998) and on the taphonomic grades of fossil bones (Sahnouni et al., 2013), the sediment studies aided in obtaining a complete picture of the sedimentary context enclosing the Oldowan occurrences excavated in this key Early Pleistocene site in North Africa. In addition, the results of the sediment and micromorphological studies are corroborated with data emanating from taphonomic and paleoecological investigations previously undertaken at the site. The implications on reconstructing Oldowan hominin behavioral patterns are also highlighted.

2 SITE BACKGROUND, STRATIGRAPHY, AND DATING

2.1 Site Background

El Kherba is situated in the Ain Hanech area on the edge of the eastern Algerian High Plateaus in the Sétif Province (**Figure 1A**) 7 km northwest of the city of El Eulma at the southern limit of the Neogene Beni Fouda sub-basin in a sedimentary outcrop cut by the deep ravine of the intermittent Oued Boucherit (895 m a.s.l.). The archeological site is located at 960–970 m a.s.l. on the northeast–southwest escarpment of Guelta Zerga (100 m higher) created by the fluvial networks of Oued Deheb that flows toward the Mediterranean. Morphostratigraphically, the site represents the end of the filling of the tertiary continental Beni Fouda sub-basin by fluvial channels carrying sediments from the margins of the Tellean formations made of gravels, sands, and floodplain muds, forming alluvial plains draining to the southwest toward the El Eulma area.

The site was discovered in 1992 following new investigations launched in the Ain Hanech research area (Sahnouni, 1998; Sahnouni and de Heinzelin, 1998). Large-scale excavations have been carried out at El Kherba yielding a rich and diverse Early Pleistocene fauna associated with Oldowan stone tools. The fauna includes Gasteropoda indet., *Mauremys leprosa*, Crocodylia indet., *Canis primaevus*, *Crocuta crocuta*, *Panthera* sp., *Felis*? *Lagomorpha*, *Elephas moghrebiensis*, *Ceratotherium mauritanicum*, *Equus tabeti*, *Equus* aff. *oldowayensis*, *Hippopotamus gorgops*, *Kolpochoerus heseloni*, *Giraffa pomeli*, *Sivatherium maurusium*, *Pelorovis howelli*, *Gazella pomeli*, and *Numidocapra crassicornis* (Sahnouni and Van der Made, 2009: Sahnouni et al., 2018). Overall, the fauna suggests a more or less open and dry landscape. However, the occurrence of a permanent body of water is indicated by the remains of crocodile, aquatic turtle, and hippopotamus. The faunal paleoecological reconstruction is supported by isotopic evidence of pedogenic carbonates indicative of a savanna ecosystem with expanding grassland vegetation and increasing aridification through time at El Kherba (Sahnouni et al., 2011).

The stone tool assemblages are made primarily of limestone and flint. They comprise cores and core-forms, whole flakes, retouched pieces, and fragments (**Figure 2**). The cores and core-forms include unifacial and bifacial choppers, polyhedrons, subspheroids, spheroids, and simple cores. The technological and typological characters show that the assemblages of Oldowan are very similar to those from Olduvai Upper Bed I and Lower Bed II in Tanzania, especially in terms of flaking patterns and resultant artifact forms (Sahnouni, 1998; 2006). Evidence, of usewear traces on several artifacts and of cut-marked and hammerstone-percussed bones, indicates that El Kherba was a place for intense subsistence activities by early hominins (**Figure 2**), including disarticulating and removing meat and breaking bones of large mammals to extract marrow (Sahnouni et al., 2013).

2.2 Regional Stratigraphy and Dating

The Sétif region is part of the Maghrebid chain formed during the alpine orogeny. It is composed mainly of marl lands of Middle Cretaceous to Neogene age (**Figure 1C**) (Djenba, 2015). The El-Eulma area, located 25 km east of Sétif, is a vast depression composed of six sub-basins (Demdoum, 2010), including the Beni Fouda sub-basin that contains the Ain Boucherit–Ain Hanech Plio-Pleistocene deposits (Duval et al., 2021). The deposits of this basin are of variable facies that consist of red clay fluvio-lacustrine sediments overlaid by heterogeneous beds of several tens of meters thick gray–yellow marls containing limestone concretions and interbedded pebbles, gravels, and sands (Demdoum, 2010). This sequence is often covered with a massive calcrete deposit that can reach 3 m of thickness in some places (Djenba, 2015).

The Oldowan site of El Kherba forms part of the Ain Boucherit–Ain Hanech Plio-Pleistocene sequence, which consists of a succession of paleontological and archeological deposits estimated to be between 4 and 1.67 Ma in age (Sahnouni et al., 2018; Duval et al., 2021). Other Oldowan localities nearby include Ain Boucherit Lower (AB-Lw), Ain Boucherit Upper (AB-Up), and Ain Hanech (**Figure 1B**). All the Oldowan deposits are encased in the 29 m thick Ain Hanech formation that comprises six stratigraphic members named, from bottom to top, P, Q, R, S, T, and U (**Figure 1D**) of fluvial origin made of alternating gravels and sandstone with mudstone (Sahnouni and de Heinzelin 1998; Sahnouni et al., 2018). El Kherba deposits were formed in Member T and slightly in the uppermost part of Member S (**Figure 3**). Member T is 4 m thick and is mainly a muddy unit, light brown (7.5 YR 6/4) or pink (7.5 YR 7/4) in color with carbonated nodulations in its final 2 m. Based on magnetostratigraphy, ESR dating, and biochronology of large mammals (proboscideans, equids, and suids), Ain Hanech and El Kherba deposits date to 1.78 Ma (Parés et al., 2014). The AB-Lw and AB-Up Oldowan deposits, situated lower in the stratigraphy, date to 2.44 Ma and 1.92 Ma, respectively (Sahnouni et al., 2018; Duval et al., 2021).

2.3 Site Stratigraphy

El Kherba stratigraphy is studied in three profiles within the excavation set out altimetrically so that the site stratigraphy can

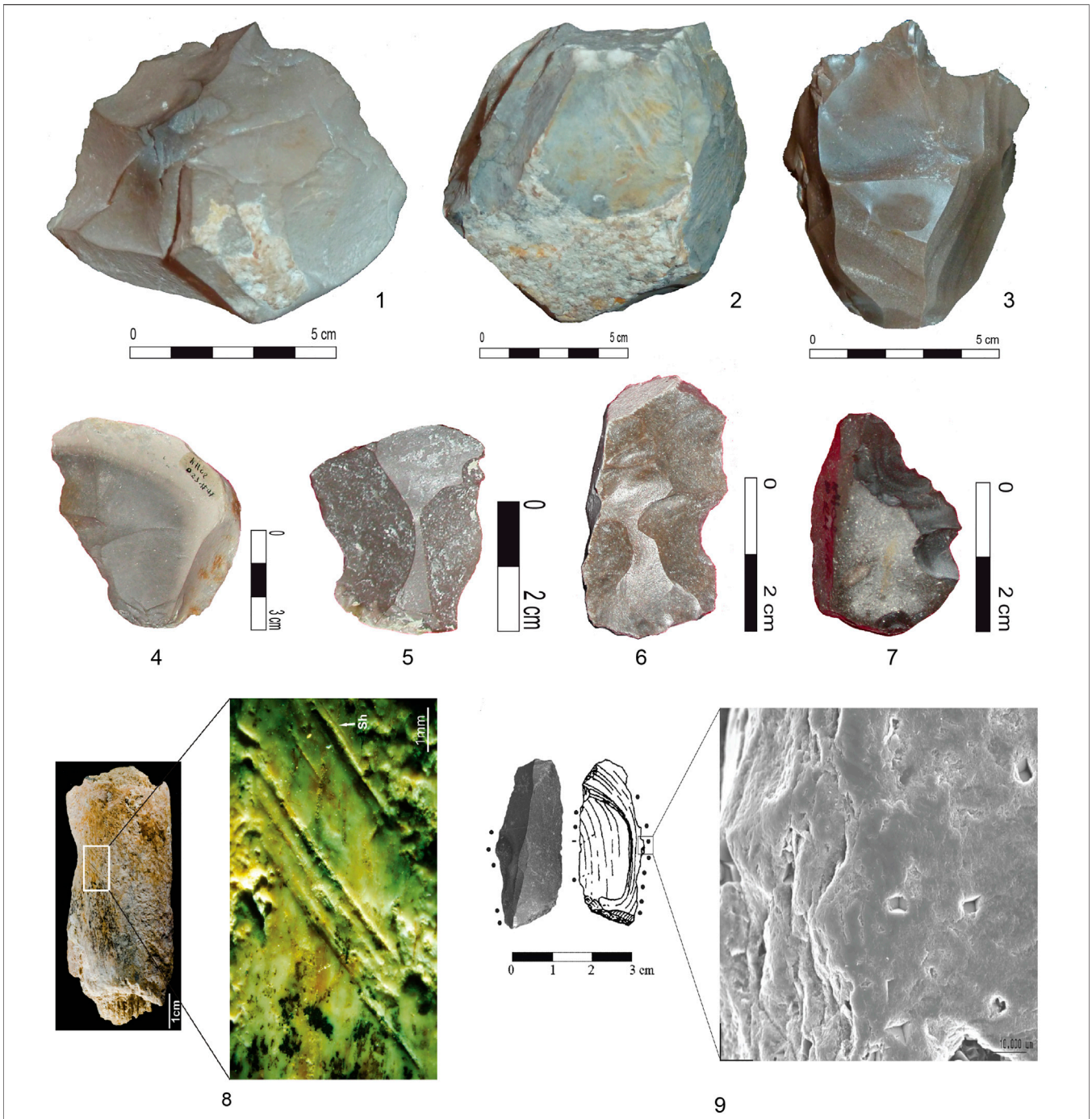

FIGURE 2 | Oldowan stone tools made of limestone and flint and an associated fossil bone from the Early Pleistocene site of El Kherba (Algeria), including (1) a bifacial chopper, (2) a polyhedron/core, (3) a core, (4–6) whole flakes, (7) a denticulate-like retouched piece, (8) a hippopotamus cut-marked rib fragment, and (9) a whole flake with evidence of usewear in cutting meat.

be described in its entirety from top to base. These include deposits in quadrant T29 of Block II (1.90 m thick), in quadrant X32 of Block II (0.90 m thick), and in quadrants N32–N33–N34–N35 (2 m thick) of Block I (**Figure 3**, Supplementary Figure S2). The correlation of these three profiles allowed us to compose a synthetic stratigraphic log of 4.80 m thickness in which 11 layers have been recognized (**Figure 3**) based on sediment texture, consistency, and color. Additional criteria were also considered in discerning the layers including proportion and granulometry of coarse elements and their nature and degree of wear and alteration, paleontological content, and, if necessary, crusting, bioturbations, and metallic

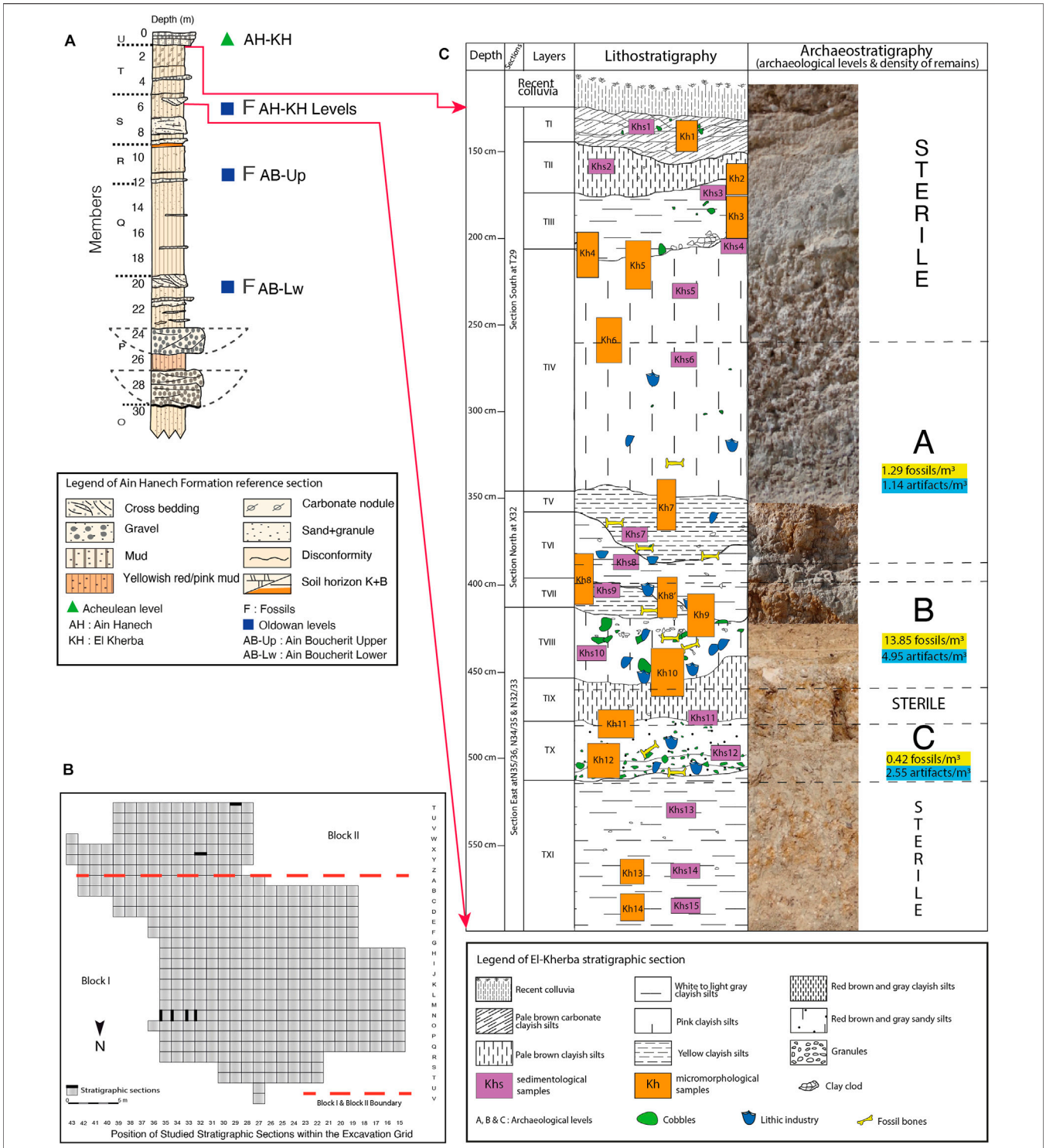

FIGURE 3 | El Kherba site stratigraphy including **(A)** position of El Kherba deposits within the Ain Hanech formation, **(B)** position of studied stratigraphic sections within the excavation grid, and **(C)** detailed stratigraphic profile and location of sampling for sediment and micromorphological studies.

inclusions (iron and manganese). The sedimentary features of the successive layers (TI–TXI), from top to bottom, are as follows.

Layer TI consists of pale brown (10 YR 8/3) homogeneous carbonated clayey silt, which is variably thick (19–27 cm), organized in sheets, friable, and strongly disturbed by rootlets from overlying colluviums; fissures that are horizontally oriented; few small-sized limestone gravels (~3 cm in diameter); and rare black flint granules. Layer TII is variably thick (15–30 cm)

consisting of compact and indurated pale brown clayey silt (10 YR 8/3) and few flint granules. Layer TIII consists of 30 cm thick indurated white gray (7.5 R 7/0) clayey silt and some medium-sized (3–6 cm) limestone pebbles. Horizontal and vertical cracks caused its disintegration in thin plates, and cracked clay clods of various sizes (8–10 cm) appear at the base. Layer TIV is 1.10 m thick pink (7.5 YR 8/4) clayey silt with fine sands in its base. The color of the sediment is heterogeneous due to $CaCO_3$ spots of variable shapes and sizes (1–5 cm), the consistency is friable, and the texture is polyhedral, flint granules. Layer TV is variably thick (10–40 cm) and bowl shaped, which consists of light reddish brown clayey silt (5 YR 6/3) with some gray clay blots (7.5 R 7/0). Fine sand is more important than in upper layers; the consistency is friable and the structure is in prismatic blocks due to vertical cracks; presence of carbonated nodules (~1 cm in diameter); this layer is poor in coarse elements. Layer TVI is thicker on the distal ends (40 and 52 cm) than in the middle (23 cm), consists of gray clayey silt (7.5 YR 7/0), has low proportion of sand, is friable and in prismatic blocks, is dotted with $CaCO_3$ spots and with metal oxyhydroxides in the form of dendrites, and has rare coarse elements. Layer TVII is 40 cm thick. It consists of light reddish brown clayey silt (5 YR 6/3) and gray clay clods (7.5 R 7/0) with fine sand, is friable and in prismatic blocks, and includes metal oxyhydroxides as veneers and carbonate spots. This layer discontinues abruptly toward the west due to a phase of erosion caused probably by a brief intensity storm event. Layer TVIII is 0.45 m thick sandy silt with a large proportion of medium-sized (3–6 cm) and large-sized (6–10 cm) pebbles and granules representing 50% relative to the fine-grained fraction. It consists of small polyhedral blocks due to numerous vertical cracks and is friable and covered with metal oxyhydroxides in the form of spots and 4–5 cm thick layers, giving it variegated color made of gray (7.5 R 7/0) and reddish brown (5 YR 6/3). Layer TIX is 0.25 m thick gray (7.5 R 7/0) and reddish brown (5 YR 6/3) variegated clayey silt with a structure organized in polyhedral aggregates. It is friable and of heterogeneous color due to metal oxyhydroxides in the form of centimetric beds and $CaCO_3$ spots and contains rare granules. Layer TX is a light gray clayey silt (2.5 Y 7/0) extending over a homogeneous thickness (0.32 m), with the presence of Mn beds (~10 cm thick) and whitish $CaCO_3$ spots. The sediment is indurated and fissured, and abundant small (1–3 cm) limestone pebbles (some of which are altered) are primarily concentrated at the bottom of the layer representing more than 70% of the deposit. Layer TXI is 0.90 m thick friable clayey silt breaking down into small polyhedral blocks due to vertical and horizontal cracks. Its color is light reddish brown (5 YR 6/3) and gray (7.5 R 7/0) with some $CaCO_3$ spots but in a lesser proportion than in the upper layers; few granules are concentrated in the middle of the layer.

In terms of associated archeological remains, fossil bones and stone artifacts are contained throughout the stratigraphy in three distinct levels, namely, from bottom to top, C, B, and A (**Figure 3**) (Sahnouni et al., 2002). They are encased in layer TX for level C; in layers TVIII and TVII for level B; and in layers TVI, TV, and the lower half of TIV for level A. The thickness of levels C, B, and A is variable including 0.55 m (depth, −483 to −538 cm), 0.62 m (depth, −398 to −460 cm), and 1.27 m (depth, −260 to −387 cm), respectively. Level B is the thinnest, yet it encases the bulk of the archeological material (18.80 finds/m^3)) (**Figure 3**).

3 METHODS

3.1 Sedimentology

Of fifteen samples (**Figure 3**), thirteen unconsolidated sediments were analyzed. Each raw sample was previously dried at 40°C before quartering. The coarse elements (gravels and pebbles) were separated by water sieving to retain only the particles <2 mm (coarse and fine sands, silts, and clays). The latter were subject to a sedimentological analysis including grain size analysis, carbonate quantification, and pH measurement. However, a brief microscopic observation of the thin sections prior to the particle size analysis revealed the presence of micritic aggregates and localized areas slightly to strongly cemented by micritic calcite. Therefore, it was necessary to use a solution of hydrogen peroxide to destroy the organic matter and 10% diluted hydrochloric acid to remove the carbonates. Then, sodium hexametaphosphate at 5 g/l was added to the sediment that was ultrasonicated for 30 s. The grain size analysis of the decarbonated sediments was carried out wet with the granulometer Malvern Mastersizer 2000 laser diffraction particle size analyzer, using the wet technique because of the silty clayey texture of the samples. In our protocol, we favored the Fraunhofer approximation because it allows for the analysis of heterogeneous sediments with different refractive indices. To optimize the reproducibility of the results, four tests were undertaken on the same sample. The results show no variation in the data and display a perfect superposition of the graphs. The average of the different results was retained. The curve and the grain size parameters were acquired in digital form. The grain size distribution of the samples was processed with the GRADISTAT software (Blott and Pye, 2006).

For estimating the carbonate proportions by infrared spectroscopy, we favored the pellet preparation method because it allows for a quantitative analysis. The employed procedure is that by Fröhlich and Gendron-Badou (2002) that includes the following steps: 1) mechanical grinding of the raw sediment with agate mortar until particles <2 μm are obtained; 2) taking 1 g sample composed of 2.5 mg of ground sediment and 997.5 mg of KBr (potassium bromide), with 10–5 g accuracy; 3) homogenization of the mixture with agate mortar during 5 min; 4) pelleting of 300 mg of the mixture under 10 to 11 tonnes of vacuum pressure during 1:30 min; 5) steaming the pellets for 24 h at 100°C to evacuate atmospheric water; and 6) measuring with an infrared spectrometer.

The pH measurement is realized with a pH meter comprising an electrode and an electronic box. 20 g of <2 mm diameter raw sediment from each sample is diluted in 50 ml of distilled water. The solution is then subjected to magnetic stirring for a few minutes. After calibrating the pH meter with neutral (scale 7), acid (scale 4), and then basic (scale 9) buffer solutions, the electrode is rinsed with distilled water and then introduced

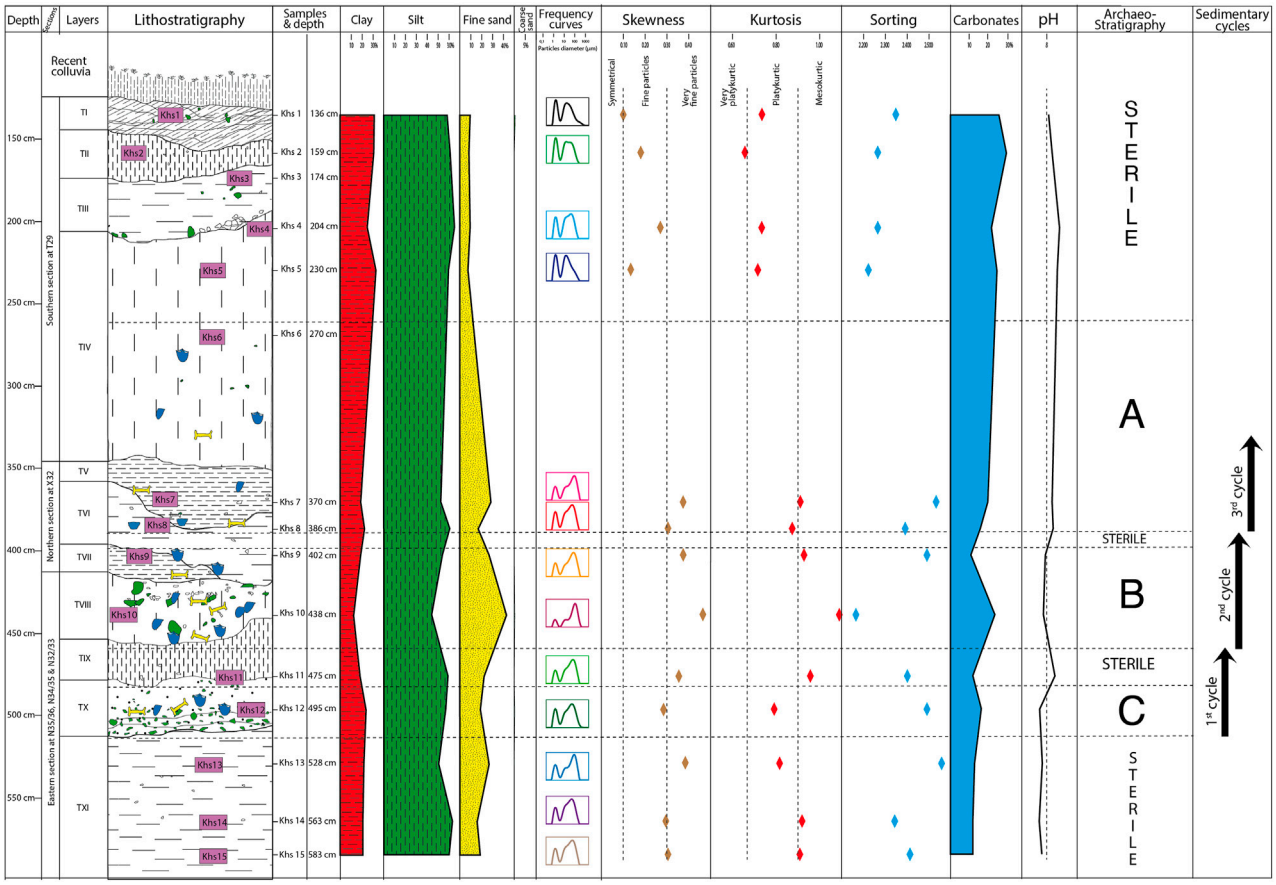

FIGURE 4 | Sedimentological results including grain size showing proportions of fine particles, frequency curves, kurtosis, skewness, sorting, carbonates, pH, and sedimentary cycles.

into the solution. The pH value is directly displayed on the electronic box screen.

3.2 Micromorphology

Fifteen micromorphological samples were collected throughout the El Kherba stratigraphic profile (**Figure 3**). The sampling procedure used is that of plaster blocks described by Courty and Fédoroff (2002), which prevents any disintegration of the sediment during its transport. In the field, the procedure consists of extracting samples in the form of blocks measuring 15 × 10 × 10 cm. The blocks can contain one or more stratigraphic layers depending on the thickness of the latter. All the visible faces of the block were plastered and labeled by site and number, stratigraphic position, and orientation. Once hardened, the blocks were removed, and their internal faces were plastered.

In the laboratory, the process developed by Guilloré (1985) was used to produce thin micromorphological sections. The blocks were opened on only one side, oven-dried at 25°C for 72 h, and cell impregnated with a mixture of polyester resin fluidized with styrene in a proportion of two-thirds/one-third, to which a few milliliters of the Butanox catalyst and 2–3 drops of an accelerator were added. They were indurated in an airy fume cupboard until the resin was completely consolidated. Each block was cut lengthwise into two parts using a diamond saw. While one part is archived as copy, the other part is cut into a 60 mm × 120 mm x 10 mm slab and mounted on a slide glass with polyester resin and thinned to 35–40 µm (for mineral transparency). A total of thirty thin micromorphological sections were made. They were first examined under a petroscope (which offers a wide field vision of the sample constituents) and then under the polarizing microscope at ×1.6, ×5, ×10, ×20, and ×63 magnifications. Plane-polarized light (PPL) and crossed-polarized light (XPL) were used for detailed description of the sediment microstructure and for taking microphotographs at various scales.

4 RESULTS

4.1 Grain Size, Carbonates, and pH Analyses

The particle size analysis reveals that El Kherba sediments are made up of a high proportion of silt–clay (80%). Sands, averaging 20%, are represented exclusively by fine sands (99%), while clays are significantly less abundant than silts (23 versus 57%) (**Figure 4**). The latter are relatively stable throughout the

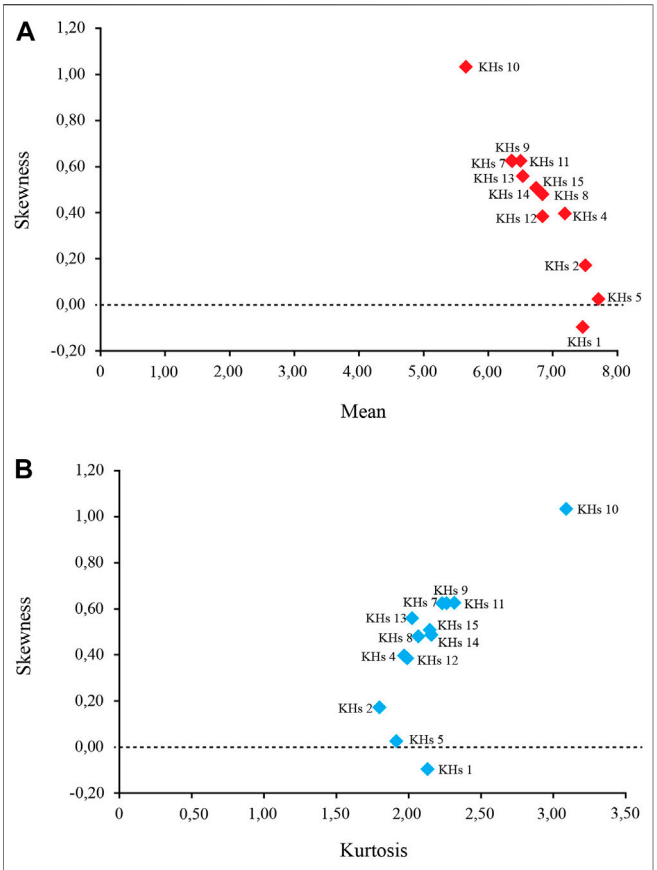

FIGURE 5 | Diagrams comparing indices (in phi), including **(A)** comparison of mean with skewness and **(B)** comparison of skewness with kurtosis.

stratigraphy, while the sands experience significant variations between the lower part of the stratigraphy (from base up to layer VIII) where they vary between 17 and 43% and the upper part (from layer VIII to the top) where they decrease to 8%. This reduction occurs mainly at the expense of clays, which gradually increase to reach 30% in the upper layers due to a change in the deposition dynamics. Based on Blott and Pye (2006) criteria, the grain size curves are bimodal in eleven samples and trimodal in the samples KHs 2 (layer TII) and KHs 10 (layer TVII). The kurtosis index ranges between 0.65 and 1.09. The highest values are in the lower part (from the base to −370 cm) showing mesokurtic and platykurtic curves. The lowest values are found toward the top part forming mostly platykurtic curves (except sample KHs 2 that is very platykurtic). According to Miskovsky and Debard (2002), all these curves reflect a mixture of one or more sediment populations. Asymmetry (or skewness) shows a tendency toward finest particles in the first half of the infilling and toward fine particles in the second half (**Figure 4**). Only sample KHs 1 presents a symmetrical curve. The sorting index, whose values are between 0.170 and 0.223, also subdivides the profile into two sets (**Figure 4**) and indicates a good sediment classification with particles increasingly calibrated toward the top. The ratio of the asymmetry (skewness) and the mean of the grains, on the scale of ϕ (**Figure 5A**), shows that all the samples, except KHs 1, have positive values. According to Friedman (1961), they correspond to sands of dunes or rivers. Yet, as these values are <1.49 ϕ, a dune origin is ruled out. The ratio of skewness and kurtosis also shows positive values (1.79–3.08 ϕ) and a wider distribution of kurtosis points (**Figure 5B**). These values also reflect sand from dunes or rivers (Friedman, 1961). Solely KHs 1 has a negative value, which is a sample from a level relatively rich in coarse sands (**Figure 4**). However, the composition of the sediments, consisting predominantly of fine particles (<40 μm), the notable proportion of fine sands (up to 43%), poor particles' sorting, and the presence of stratification suggest hydric deposition of the sediments. However, the presence in some samples of more than one mode does not rule out an eolian origin of the sands.

The carbonates are nodules of a few centimeters in diameter, or in the form of cement. Infrared spectroscopy analysis of the raw sediments indicates that their proportion varies between 11 and 30% with the lower part of the deposits being less supplied (**Figure 4**). Their evolution, which is close to that of fine sands in the lower half of the infilling, becomes, thereafter, parallel to that of the clays in the upper half. This concomitant evolution of carbonates and sands in the lower layers shows a common detritic origin of the two fractions, while in the upper layers, they are in a secondary position following the recrystallization of the calcite within the mass (see *Micromorphological Analysis*).

The sediments have an alkaline pH with minor values (7.66–7.94) in the lower levels of the infilling than in the upper levels (8.09–8.59) (**Figure 4**). Their evolution is related to carbonates, which allows carbonate stability (Karkanas and Goldberg, 2019) and creates favorable conditions for a good preservation of faunal remains (Stephan, 2000; Berna et al., 2004; Karkanas, 2010). Despite the alkalinity of the sediments, we note the presence of some organic residues, which require a humid environment and an acidic pH~3 (Fraysse et al., 2004; Shahack-Gross et al., 2004). This antinomy is explained by the contribution of water rich in calcium carbonate transforming the acidic medium into a basic medium (Shahack-Gross et al., 2004) and would have contributed significantly to the decomposition of organic matter (Karkanas, et al., 2000; Fraysse et al., 2009).

To sum up, El Kherba grain size data reveal a stability in the evolution of the proportion of silts and variations in those of sands and clays depending on the depth of the stratigraphic profile. These differences allow us to subdivide the profile into two sedimentation phases. The first phase, from the base to −370 cm, is somewhat high-energy deposit as it is formed of a coarse fraction of pebbles and granules along with a fine fraction comprising 56% silt and 24% sand. The second phase, which extends to the top of the profile, is relatively stable and characterized by more homogeneous sediments and a silty clayey texture (61% silt and 30% clay). The different parameters (kurtosis, skewness, sorting) confirm this subdivision with distinct values in the two parts of El Kherba stratigraphy suggesting two modes of deposition. The first mode characterizes its lower part that is silty–sandy with a high concentration of gravels and cobbles. These deposits correspond to alluvium of bottom load generated

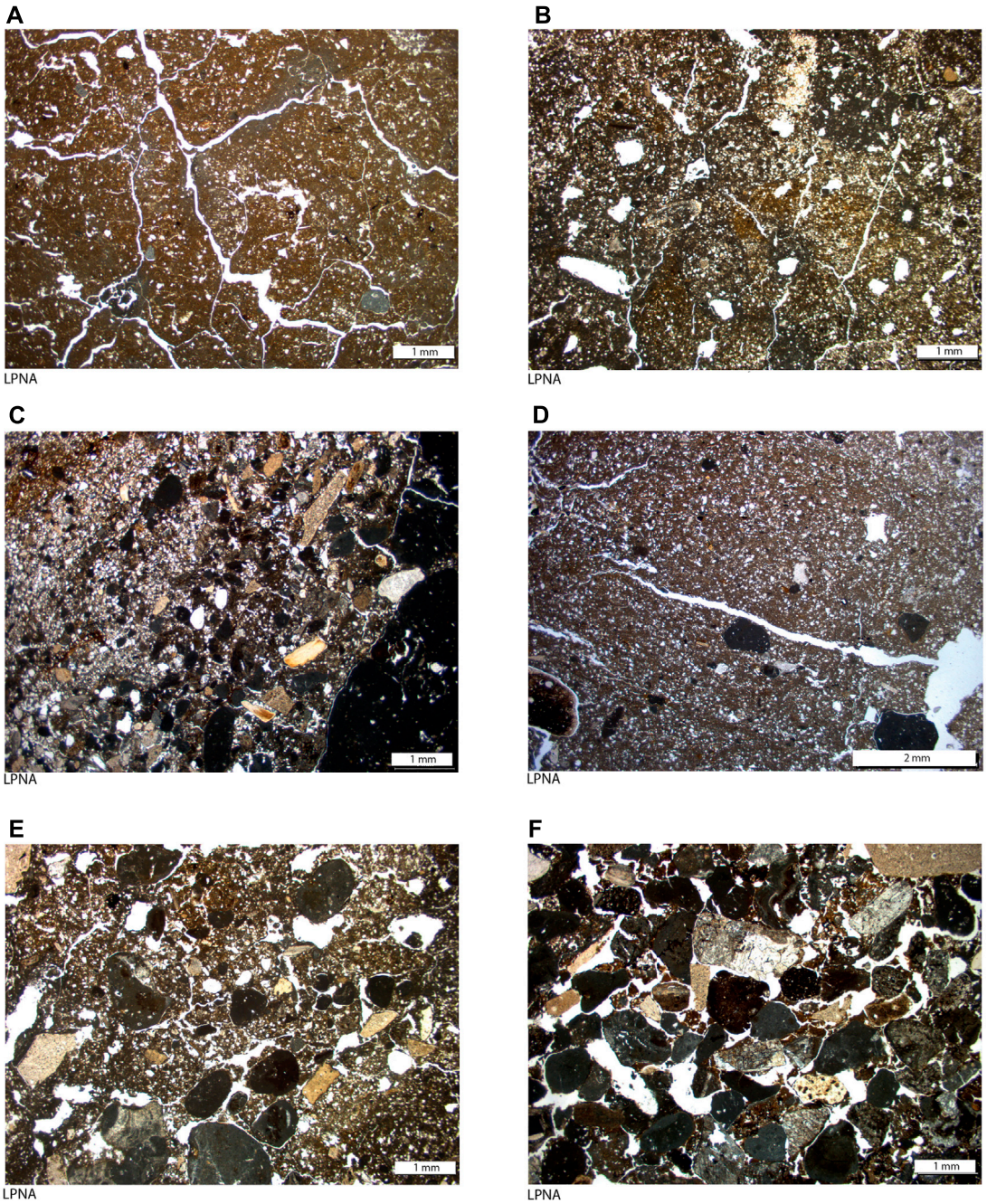

FIGURE 6 | Sedimentary facies including **(A)** clayey silty microfacies with a massive structure and subangular polyhedral blocks, separated by splits and deviated and interconnected cracks typical of the shrinking–swelling phenomenon (sample KH 1B, layer I); **(B)** a microstructure with subangular polyhedral blocks superimposed on a microstructure with channels invoking a rootlet biological activity (sample KH 3B, layer III); **(C)** microfacies with bedded microstrata of coarse and fine sands (sample KH 12H, layer X); **(D)** microfacies with compact silty–clayey–sandy lenses superimposed on silty–sandy lenses with a platy microstructure (sample KH 7B, layer V); **(E)** microfacies with unorganized and heterogeneous coarse particles with grain and micro-aggregate packing, plane voids, and porphyric distribution (sample KH 2H, layer II) and **(F)** with chitonic distribution (sample KH 12H, layer X).

by a high-energy regime. The second mode concerns its upper part, which consists of an exclusively silty clayey texture suggesting an attenuation of the intensity of the water regime with the deposition of fine particles. Fine-grained particles and the alternation of lenses of fine sands and silts (see *Micromorphological Analysis*) rather suggest their transport by low energy currents and their settlement by suspension during periodic flooding characteristic of floodplain setting, which is known to be deposited at lower flow speeds.

4.2 Micromorphological Analysis

The micromorphological features of the El Kherba sediments are summarized and comprehensively described with their paleoenvironmental implications, respectively, in **Supplementary Table S1** and Supplementary Text (**Supplementary Material**). Here, we highlight the results of the micromorphological study concerning the lithological facies and post-depositional development of the sediments.

4.2.1 Lithological Microfacies

Based on the micromorphological study, three lithological microfacies are recognized in El Kherba, which are repeated throughout the stratigraphic profile. The first microfacies is clayey silt with a massive structure approaching 85–95% of the total sediment. This high proportion of the fine fraction, unorganized and devoid of coarse elements, characterizes flood plain sediments deposited by suspension (Courty and Féderoff, 2002) and assumes a slow burial (Vallverdú et al., 2001). The texture of this facies also constitutes an impermeable layer conducive to water retention. As a result of its drying up during the dry seasons, a microstructure is formed with subangular polyhedral blocks, separated by planes and cracks deviated and interconnected slots (**Figure 6A**) typical of the shrinking–swelling phenomenon (Courty et al., 1989). When the biological activity is expressed, the microstructure with subangular polyhedral blocks then overlays a microstructure with channels (**Figure 6B**). The distribution is in both cases porphyric. Depletion pedofeatures are expressed by the loss of the fine fraction and the on-site concentration of the coarse residues. They are indicative of significant water circulation (Berger et al., 2012).

The second microfacies is made of bedded microstrata of coarse and fine sands (**Figure 6C**) or of compact silty–clayey–sandy microstrata overlaying sandy–silt lenses with a platy microstructure (**Figure 6D**). The plane porosity is sub-horizontal to horizontal and occurs at the junction of sandy and silty beds. The alternation of these microstrata with compact structures results from a change in water flow sedimentation by spreading in a calm environment generated by low-velocity runoffs. The preservation of these silty–sandy lenses is explained by the rapid burial of the sediments (Vallverdú et al., 2001).

The third microfacies is related to heterogeneous unorganized coarse particles illustrating the unexpected character of the sedimentation (Vallverdú et al., 2001). They denote an increase in the water regime and particle fining upward suggesting a diminution in the water velocity (**Figure 6C**). The microstructure is stacked with grains and micro-aggregates with plane voids. The distribution is often porphyric, that is to say, these elements are included in the fine matrix (**Figure 6E**). When fine material is piled up in the intergranular porosity or forms films around the particles (**Figure 6F**), the distribution is called chitonic. These coarse particles are clasts, rounded micritic aggregates, iron–manganese and carbonated nodules, and numerous terrestrial shell remains.

4.2.2 Post-Depositional Development

The pedologic processes that affected El Kherba sediments include cracking of deposits, coatings, recrystallization of carbonates, impregnation of metal oxyhydroxides, and rootlet bioturbations. Cracking of deposits corresponds to post-infilling restructurations. They can be structural, mechanical, or biological. When structural, the cracking of deposits characterizes the coarse layers. The mechanical movements are due to the plastic deformations of the matrix, which occur during the alternation of the wetting and drying phases (Courty et al., 1989). They generate a porosity with deviated planes in the clayey silty or plane accumulations in the bedded layers. Subsequently, the voids were filled, partially or totally, with fine sand (**Figure 7A**) or heterogeneous sediment aggregates (**Figure 7B**) coming from paleosurfaces or resulting from disturbance of existing layers. The biological porosity is caused by the development of rootlets.

The coatings concern voids and aggregates on the one hand and rootlet vughs on the other hand. The first are related to post-sedimentary illuviation (Jamagne et al., 1987) and are made up of colloids or silty particles. Colloids are of two types: limpid and dusty. Limpid colloids are microlaminated and cover the interior of voids (**Figure 8A**) or wrap minerals (**Figure 8B**). They come from the dismantling of paleostructures and are attributed to medium energy water circulation (Fédoroff and Courty, 1994), and their mode of deposition is mainly made by capillarity in an environment characterized by contrasted alternating wet and dry seasons (Fédoroff, 1997). When the colloids contain silty particles, they become dusty and brown (**Figure 8C**) suggesting higher water circulations (Fédoroff and Courty, 1994; Jongmans et al., 2001; Kühn et al., 2010) or leaching of the fine fraction (Curmi, 1987). The second type of coating deals with rootlet porosity and is characterized by a regular and compact coating, often parallel to the major axis of the vugh (**Figure 8D**). It can reach up to 300 μm in diameter and consists of a decarbonation residue resulting from the dissolution of limestone by the rootlets during their development (Favre, 1937; Lucas and Montenat, 1967; Jaillard and Callot, 1987). The papules (**Figure 8E**) are small fragments of limpid clay from old clay illuviations and integrated into the groundmass. Their fractionation is due to the alternation of shrinking–swelling cycles, which occur during the wet–dry seasons (Kühn et al., 2010).

The carbonates appear in the form of micritic calcite or millimetric nodules. The latter are exogenous and numerous in the lower stratigraphic layers, and their origin and evolution are comparable of those of sands (**Figure 4**) as a result of dismantlement of catchment areas and their subsequent transport. The micritic calcite is secondary. Its diffusion in the mass also evolves in the same direction as the silty clayey fraction and passes from borders lining some cracks and micritic aggregates of the lower part of the stratigraphic profile (**Figure 9A**) from partial to total impregnation of localized areas in the upper part (**Figure 9B**). The formation of this cement presumes a humid environment and a neutral to basic pH (Mallol et al., 2017) resulting from inputs of water rich in calcium

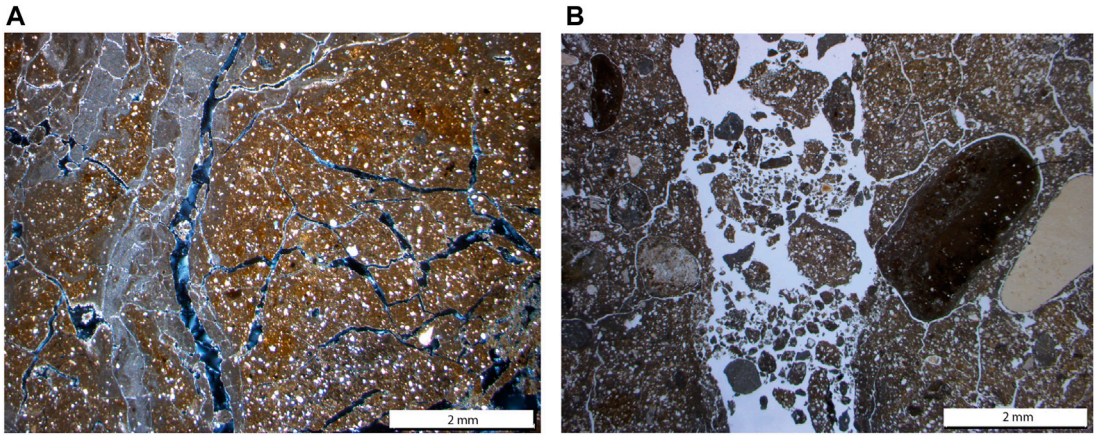

FIGURE 7 | Cracking of deposits including **(A)** partially or completely filled cracks with very fine sand (sample KH 5B, layer IV) and **(B)** deposition by illuviation or heterogeneous aggregates (sample KH 4B, layer IV).

carbonate combined with a low permeability of silty clayey layers. The saturation of the waters with calcium carbonates causes calcite precipitation when the water table dries out. The precipitation of calcite (Picq et al., 2002) accumulated in the form of micrite in the sediments and crusting around large mammal bones preserving them from erosion. As Freytet and Verrecchia (1989) pointed out, it is very likely that certain carbonate nodules can be derived from the fractionation of this micrite.

The impregnation of metallic oxyhydroxides is characterized by coatings (**Figure 10A**), by hypocoatings (**Figure 10B**) of voids, or in the form of edgings (**Figure 10C**). They reflect hydromorphic conditions, which involve redox cycles. These suppose 1) flooding of the deposits creating a reducing setting releasing iron and impoverishment of the zones (gray color of the matrix) and 2) during the drying up of the water, a transition to an oxygenated setting during which iron permeates the sediment (orange color of the matrix) (Courty et al., 1989). These recurring iron concentrations suggest the existence throughout the stratigraphic profile of several episodic phases of waterlogging and drying up of the deposits, and they are all more manifested when the sediment is fine-grained and less permeable and also participate in the process of iron reduction during their decomposition by micro-organisms (Karkanas and Goldberg, 2019). These features are detailed in the work by Le Drészen (2008) in the Sahel region, who equated the diffuse impregnation to dehydration of the sediments and the ferruginous borders to drying up of ponds. As for the double coatings, the ferri-argilanes, observed in rootlet voids (**Figure 10B**), are explained by the dissolution and leaching of carbonates from the fine fraction followed by iron precipitation (Massenet, 2008).

Bioturbation features are of moderate intensity represented by terrestrial shell remains and rootlets. However, rootlet bioturbations are more manifest and materialized by channels and pores, whether or not containing plant residues. These are calcified rootlets (**Figure 11A**) or rootlets (probably grasses) in the process of decomposition (**Figure 11B**). These rootlets consist of a mosaic of nested cells, roughly rounded or polyhedral averaging 25 µm in diameter. Organic matter is mainly expressed in the fine-grained layers, which implies that these have been saturated with water for at least part of the year (Jaillard, 1992). When this water regime evolves toward a reducing setting, there is iron precipitation and/or manganese oxides around the rootlet voids (Karkanas, 2010; Chen et al. (1980). Such features are present in certain voids of El Kherba sediments in the form of a single coating (**Figure 10A**) or superimposed on clay illuviations (**Figure 10B**). The plants from which these residues emanate usually develop under meadows, Mediterranean or alpine environments (Jaillard et al., 1991). However, an open savannah ecology is also in good agreement with the formation of these structures (Jaillard, personal communication).

5 DISCUSSION

The results of the sediment and micromorphological studies reported here allow us to discuss the implications of El Kherba sedimentary context in relation to the integrity of the Oldowan assemblages and their potential for preserving hominin behavioral information. As mentioned above, El Kherba sediments preserve traces of repeated Oldowan occupations, which are concentrated in three archeological levels, namely, from top to bottom, A, B, and C (**Figure 3**) (Sahnouni et al., 2002). Level C is correlated with the upper part of layer TXI and layer TX; level B is correlated with layers TVIII and TVII; and level A is associated with layers TVI, TV, and the lower half of TIV. Points of interest that need to be discussed here include 1) the type of depositional environment in which the hominin activities took place and 2) the impact of the depositional processes on the integrity of El Kherba Oldowan remains. With regard to the depositional environment, the grain size analysis of fine particles <2 mm clearly shows that the archeological levels are encased

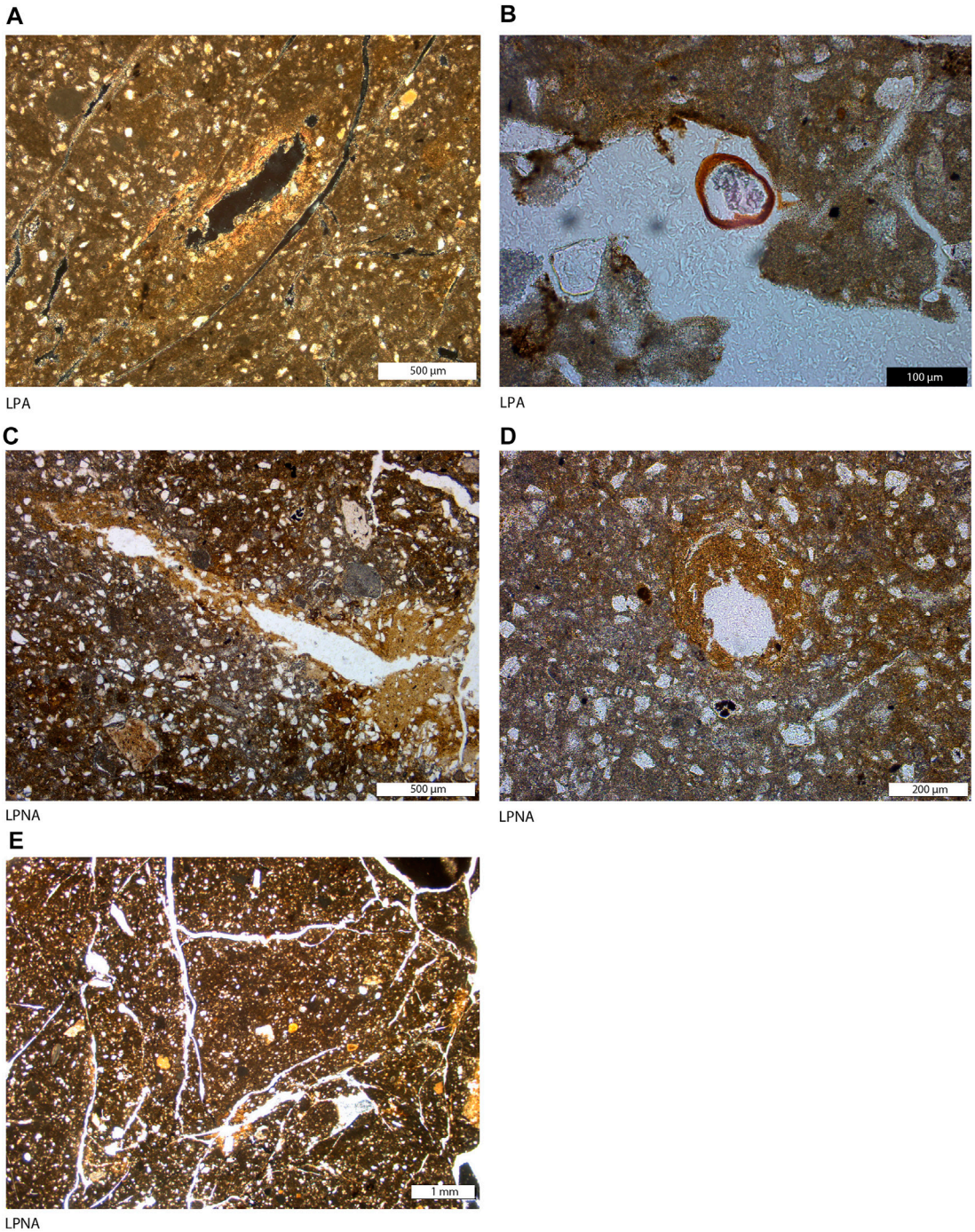

FIGURE 8 | Coatings including **(A)** microlaminated colloids covering the interior of voids (sample KH 6B, layer IV) and **(B)** surrounding aggregates that are to be linked to post-sedimentary illuviation (KH 4B, layer IV). **(C)** When the colloids contain silty particles, they become dusty or impure reflecting higher water circulations (KH 4B, layer IV). **(D)** In root porosity, the coatings are regular, compact, and often parallel to the major axis of the vugh formed by a decarbonation residue (sample KH 14, layer XI). **(E)** The papules are small fragments of limpid clay from old clayey illuviation and integrated into the basal mass (KH 6B, layer IV).

predominantly in fine-grained particles including silt, clay, and fine sand. On a microscopic scale, fine sands are often bedded, whereas the silts are massive and rarely microstructured. Thus, the archeological deposits were formed during sedimentary cycles with graded bedding in which each level begins with coarse sediments and is overlaid by finer particles or massive silts. This rhythmicity corresponds to hydro-sedimentary cycles where water flow was the main factor of transport and settling out of sediment grains. Notwithstanding the presence of coarse elements, the environment during the settling out of these deposits is temperate. It is widely

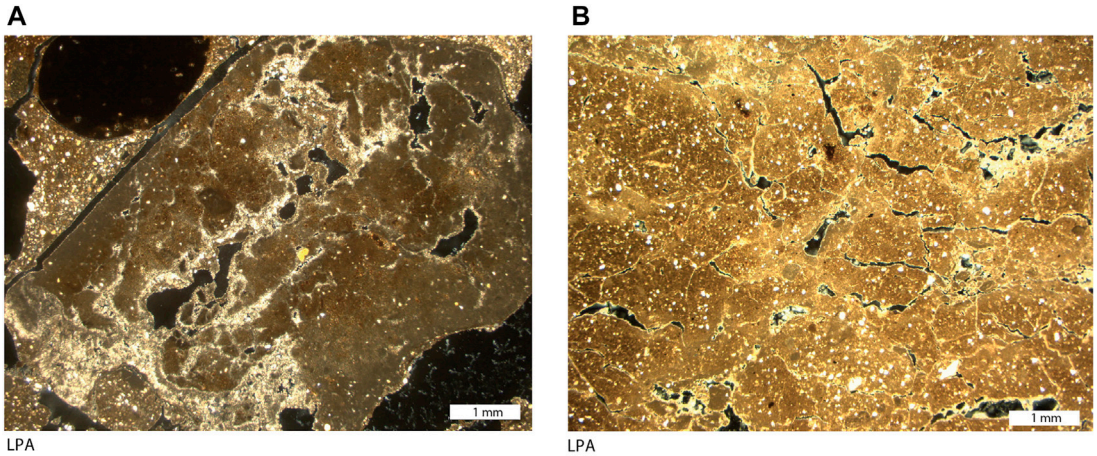

FIGURE 9 | Carbonates extend from **(A)** borders covering cracks and micritic aggregates in the lower levels (sample KH 11, layer IX) to **(B)** a partial to total impregnation of deposits toward the top (sample KH 1B, layer I).

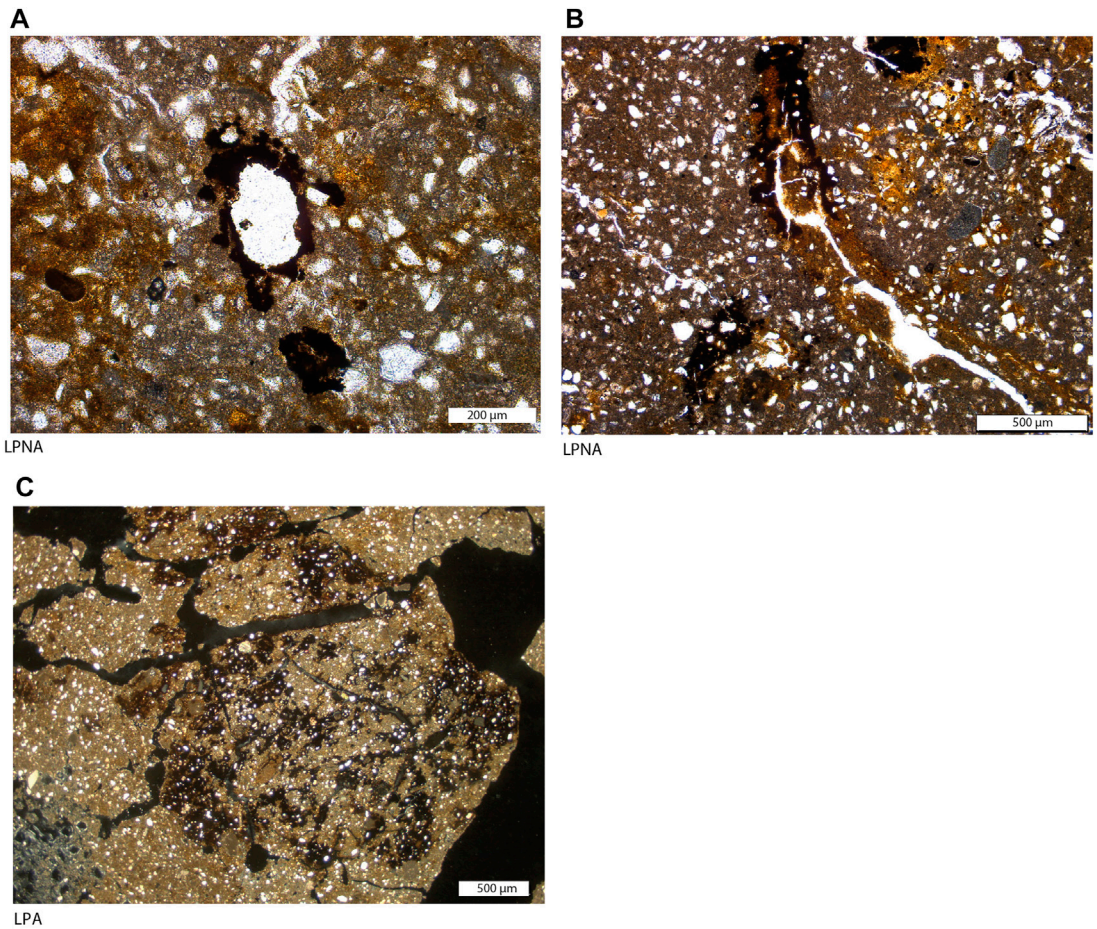

FIGURE 10 | Metallic oxyhydroxide characteristics, including **(A)** coatings (sample KH 14, layer XI) or **(B)** hypocoatings of void (sample KH 7H, layer IV) and **(C)** impregnations in the form of edgings (sample KH 10H, layer VIII). The types **(A, B)** reflect hydromorphic conditions which involved oxidation–reduction cycles. The double coatings (ferri-argilanes) observed in rootlet voids **(B)** are explained by the dissolution and leaching of carbonates from the fine fraction followed by iron precipitation.

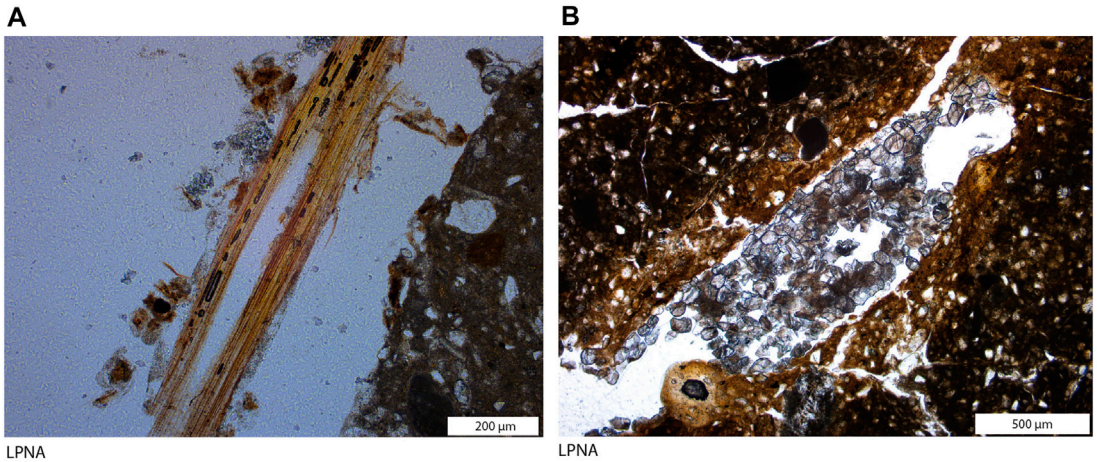

FIGURE 11 | Plant remains including **(A)** calcified rootlets (sample KH 9H, layer VI) and **(B)** rootlets, possibly of grasses in the process of decomposition (sample 6H, layer IV).

expressed by the predominance of fine-grained sediments, which represent the undeniable mark of deposition by suspension in a floodplain environment for the massive facies and by low runoff for the bedded facies. As for the levels rich in sands and granules, they signal secondary climatic oscillations characterized by an increase in precipitation during rainy seasons.

The decline in the proportion of sands from the base to the top of the infilling and their progressive replacement by silts and clays herald a gradual transition from a temperate climate to an arid one. This change toward a dry environment is supported by the observed variations in carbonate proportions. A fraction of the carbonate has been transported and deposited with the sands, as is the case in the archeological levels where the variations of the carbonates and sand fractions are parallel (e.g., in levels C and B). The rest of the carbonates emanate from the recrystallization of the calcite (e.g., level A), contained in these flooding silts, after the drying up of the water suggesting an arid environment. The change to an arid environment is corroborated by isotopic and faunal evidence (Sahnouni et al., 2011). For instance, isotopic analysis of El Kherba pedogenic carbonates shows a strong positive trend of increasing $\delta^{13}C_{PC}$ and $\delta^{18}O_{PC}$ values through time suggesting a temporal increase in C_4 vegetation and in aridification, respectively. The faunal evidence shows the presence in the upper levels of more hypsodont bovines, an increase in the abundance of equids, and the disappearance of small antelopes more adapted to a less open habitat.

In terms of site integrity, these sedimentary structures indicate that the burial of archeological remains in fine particles preserved them from biodegradation and hydraulic disturbance forces. The impact of soil processes on sediment deposition must have been limited or of lesser intensity as shown by the microlaminations. Based on the sedimentary evidence, overall, the El Kherba archeological occurrences appear to have been buried in a primary sediment context with minimal rearrangement. Other lines of evidence, including the physical aspects of the archeological occurrences and their spatial disposition in the site, substantiate to a great extent the integrity of El Kherba Oldowan site (Sahnouni et al., 2013). For instance, the bone weathering patterns [primarily stages 1 and 2 based on criteria by Behrensmeyer (1978)] indicate that animal bones were exposed to climatic conditions for less than 3 years prior to burial. The faunal assemblage comprises all categories of skeletal elements, making hydraulic sorting unlikely. In addition, fossil bones and stone artifact show neither a preferred orientation nor a high dip (Sahnouni et al., 2013) (**Supplementary Figures 3C, Da,b**). Similarly, the lithic assemblages are macroscopically fresh and coherent and include cores, debitage, and small fragments (<2 cm of maximum dimension) (**Supplementary Figure 3A**). The debitage and small fragments are overwhelmingly represented relative to cores mimicking experimental stone tool assemblages generated by Schick (1986) (see **Supplementary Figure 3B**). In addition, a number of stone tools preserved usewear on their edges (Sahnouni et al., 2013). If these stone tools have been subject to water rearrangement, the usewear would have not been preserved. However, the preservation of the archeological material is not homogeneous across all the site. As a matter of fact, some bone fragments show various degrees of polish damage on their surfaces. These occur particularly in level B corresponding stratigraphically to layer TVIII in which a quantity of fine sands and a small amount of coarse sands are present. They might have been introduced from close distance by medium energy currents in the course of channel aggradation. According to Behrensmeyer (1982) and Behrensmeyer and Chapman (1993), abraded bones are usually found within floodplain deposits as a result of channel lateral aggradation and bone reworking through bank erosion in a fluvial system consequently to intense and intermittent rain precipitations.

6 CONCLUSION

This paper presented the sedimentary context of the Oldowan site of El Kherba (Ain Hanech, Algeria) involving sediment and micromorphological studies. The following tentative conclusions are proposed.

The studies offered a detailed assessment of the sedimentary processes that took place in the accumulation of the Oldowan remains. For instance, the grain size analysis shows that the sediments encasing El Kherba fossil bones and stone tools are primarily fine-grained particles, mainly silt and clay. Likewise, the micromorphological study reveals massive sediment structures made primarily of fine particles. The massive sediment structure is suggestive of water retention and supersaturation of the deposits making them impermeable. This type of sediment size characterizes flood basins which are known actually to be deposited at lower flow speeds. The El Kherba floodplain environment created favorable conditions for a rapid burial of animal bones and stone tools, and ultimately preserving valuable archeological data that allow us to reconstruct hominin technological and subsistence behaviors dated back to 1.8 Ma. As a matter of fact, El Kherba excavations yielded well-preserved faunal and lithic assemblages with evidence showing a clear causal link between Oldowan stone technology and processing of large animal carcasses for meat acquisition by early hominins (Sahnouni et al., 2013). The lithic assemblage incorporates all the technological stages of the sequence reduction for the manufacture of Oldowan tools and used artifacts. The bone assemblage includes all anatomical skeletal elements and several cut-marked and hammer-stone percussed bones.

The studies also contributed to the reconstruction of the prevailing environments during which early hominins carried out their behavioral activities. The microscopic study of the sediments indicates that El Kherba archeological levels were accumulated in fining-upward sediment cycles in which each level starts with coarse particles and ends up with massive silts or micro-bedded sand or silty sand. From a paleoenvironmental point of view, the sedimentary evidence overall suggests a temperate climate with increasing rainfall during rainy seasons. The decline of sands and the high proportion of carbonates from layer VI and upward is indicative of a gradual change from humid to arid environment. This environmental change is consistent with faunal and isotopic evidence of increasing open landscape and aridification documented throughout the El Kherba stratigraphic profile, particularly from archeological levels B to A with impact on early hominin foraging activities. Isotopic evidence suggests that level B was predominately closed habitat with C_3 vegetation probably in riparian settings with networks of fluvial channels (Sahnouni et al., 2011; 2017). In such habitat, rivers would have provided rocks for stone tool manufacture and would have attracted game for meat acquisition by early hominins. In contrast, the evidence suggests that, during level A, the environment was increasingly open and arid. An arid habitat would have offered much less opportunities for accessing water and food supplies due to their scarcity on the landscape. The impact of the environmental change on early hominin foraging capabilities is likely reflected in the abundance of stone tools and fossil bones in level B and their paucity in level A.

From a methodological point of view, to the best of our knowledge, this is one of the rare comprehensive inquiries into sedimentary processes that have been fully integrated in North African Lower Paleolithic studies. This sedimentary context investigation has been undertaken within a multi-perspective examination of the processes that took place in the formation of El Kherba site, which also includes taphonomic grades of bones and patterns of stone artifact concentration. This multi-perspective approach has become a standard procedure to identify the different agencies playing a role in the formation of a Paleolithic site prior to any archeological interpretation of fossil remains and stone artifact concentration patterns. The sedimentary context is a line of evidence of great interest in appraising formation processes as it provides assessment regarding possible disturbance of archeological occurrences, and it contributes to reconstructing the environment in which the hominin activities took place. The results of the sedimentary matrix analyses are consistent with those of bone taphonomy and concentration of artifacts converging to the same conclusion, that is, El Kherba Oldowan assemblages were accumulated in the primary sedimentary context although minimal rearrangement of remains might have occurred (Sahnouni et al., 2013). In addition, the sedimentological and micromorphological results are also coherent with faunal and isotope evidence regarding El Kherba paleolandscape reconstruction and environmental change (Sahnouni et al., 2011).

DATA AVAILABILITY STATEMENT

The original contributions presented in the study are included in the article/**Supplementary Material**, and further inquiries can be directed to the corresponding author.

AUTHOR CONTRIBUTIONS

SA and MS conceived and designed the study. All authors contributed to the field investigation and to the writing of the manuscript (original draft preparation, review, and editing). MS and ZH were responsible for the project administration. All authors have read and agreed to the published version of the manuscript.

FUNDING

This research was funded by UMR7194 (CNRS, MNHN) and through grants awarded to MS grant PGC 2018-095489-B-100 by MCIN/AEI/10.13039/501100011033 and MINECO (HAR 2013-41351-P)], CNRPAH (Algeria), The L.S.B. Leakey Foundation (San Francisco, CA, United States), the European Research Council (FP7-People-CIG2993581) (Belgium), and the Stone Age Institute (Bloomington, IN, United States).

ACKNOWLEDGMENTS

The authors thank the Algerian Ministry of Culture for the research permit; Centre National de Recherches Prehistoriques, Anthropologiques et Historiques (CNRPAH), the Wilaya of Sétif, the municipality of Guelta Zerga, and the University of Sétif 2 (Algeria) for administrative and logistic support during fieldwork at El Kherba; the UMR 7194 sedimentological laboratories (Paris, France) for carrying out the sedimentological and micromorphological analyses, and Xavier Gallet of the same for pellet preparation and for the infrared spectra reading; and CENIEH (Spain) staff Beatriz de Santiago Salinas and María José de Miguel del Barrio for administrative support to MS.

SUPPLEMENTARY MATERIAL

The Supplementary Material for this article can be found online at: https://www.frontiersin.org/articles/10.3389/feart.2022.893473/full#supplementary-material

REFERENCES

Behrensmeyer, A. K., and Chapman, R. E. (1993). "Models and Simulations of Time-Averaging in Terrestrial Vertebrate Accumulations," in *Taphonomic Approaches to Time Resolution in Fossil Assemblages*. Editors S. M. Kidwell and A. K. Behrensmeyer (Knoxville: The Paleontological Society), 6, 125–149. Short courses paleontol. doi:10.1017/s2475263000001082

Behrensmeyer, A. K. (1978). Taphonomic and Ecologic Information from Bone Weathering. *Paleobiology* 4, 150–162. doi:10.1017/s0094837300005820

Behrensmeyer, A. K. (1982). Time Resolution in Fluvial Vertebrate Assemblages. *Paleobiology* 8, 211–227. doi:10.1017/s0094837300006941

Berger, J.-F., Bravard, J.-P., Purdue, L., Benoist, A., Mouton, M., and Braemer, F. (2012). Rivers of the Hadramawt Watershed (Yemen) during the Holocene: Clues of Late Functioning. *Quat. Int.* 266, 142–161. doi:10.1016/j.quaint.2011.10.037

Berna, F., Matthews, A., and Weiner, S. (2004). Solubilities of Bone Mineral from Archaeological Sites: the Recrystallization Window. *J. Archaeol. Sci.* 31 (7), 867–882. doi:10.1016/j.jas.2003.12.003

Blott, S. J., and Pye, K. (2006). Gradistat: A Grain-Size Distribution and Statistic Package for the Analysis of Unconsolidated Sediments. *Earth Surf. Process. Landforms* 26, 1237–1248. doi:10.1002/esp.261

Chen, C. C., Dixon, J. B., and Turner, F. T. (1980). Iron Coatings on Rice Roots: Morphology and Models of Development. *Soil Sci. Soc. Am. J.* 44 (5), 1113–1119. doi:10.2136/sssaj1980.03615995004400050046x

Courty, M. A., and Fédoroff, N. (2002). "Micromorphologie des sols et sédiments archéologiques," in *Géologie de la Préhistoire : Méthodes, Techniques et Applications*. Editor J. C. Miskovsky (Paris: Géopré, Presses Universitaires de Perpignan), 511–554.

Courty, M. A., Goldberg, P., and Macphail, R. I. (1989). *Soils and Micromorphology in Archaeology*. Cambridge: Cambridge University Press.

Courty, M. A. (1992). Soil Micromorphology in Archaeology. *Proc. Br. Acad.* 77, 39–59.

Curmi, P. (1987). "Sur la signification des revêtements complexes argileux et limoneux dans les sols lessivés acides," in *Soil Micromorphology*. Editors N. Fédoroff, L. M. Bresson, and M. A. Courty (Paris: AFES), 251–255.

Demdoum, A. (2010). *Étude hydrogéochimique et impact de la pollution sur les eaux de la région d'El Eulma. Doctoral Thesis*. Constantine, Algeria: Université Mentouri.

Djenba, S. (2015). *Influence des paramètres géologique, géomorphologique et hydrogéologique sur le comportement mécanique des sols de la wilaya de Sétif (Algérie)*. Doctoral Thesis. Biskra, Algeria: Université Mohamed Kheider.

Duval, M., Sahnouni, M., Parés, J. M., Van der Made, J., Abdessadok, S., Harichane, Z., et al. (2021). The Plio-Pleistocene Sequence of Oued Boucherit (Algeria): A Unique Chronologically-Constrained Archaeological and Palaeontological Record in North Africa. *Quat. Sci. Rev.* 271, 107–116. doi:10.1016/j.quascirev.2021.107116

Favre, J. (1937). "Découverte de *Microcodium elegans* dans la gompholite du Haut Jura neuchâtelois. Étude de la position de cette Algue," in *Étude sur le Tertiaire du Haut Jura neuchâtelois*. Editors J. Favre, P. Bourquin, and H. G. Stehlin (Bâle: Société Paléontologique Suisse), 39–44.

Fédoroff, N. (1997). Clay Illuviation in Red Mediterranean Soils. *Catena* 28, 171–189. doi:10.1016/s0341-8162(96)00036-7

Fédoroff, N., and Courty, M. A. (1994). "Organisation du sol aux échelles microscopiques," in *Pédologie 2 : Constituants et propriétés du sol*. Editors P. Duchaufour and B. Souchier. 2nd édition (Paris: Masson), 349–375.

Fraysse, F., Pokrovsky, O. S., Schott, J., and Meunier, J.-D. (2009). Surface Chemistry and Reactivity of Plant Phytoliths in Aqueous Solutions. *Chem. Geol.* 258, 197–206. doi:10.1016/j.chemgeo.2008.10.003

Fraysse, F., Pokrovsky, O. S., Schott, J., and Meunier, J.-D. (2004). Surface Properties, Solubility, and Dissolution Kinetics of Bamboo Phytoliths. *Geochim. Cosmochim. Acta* 70, 1939–1951. doi:10.1016/j.gca.2005.12.025

Freytet, P., and Verrecchia, E. (1989). Les carbonates continentaux du pourtour méditerranéen : microfaciès et milieux de formation. *Méditerranée* 68 (2-3), 5–28. doi:10.3406/medit.1989.2613

Friedman, G. M. (1961). Distinction between Dune, Beach, and River Sands from Their Textural Characteristics. *J. Sediment. Petrology* 31 (4), 514–529. doi:10.1306/74d70bcd-2b21-11d7-8648000102c1865d

Fröhlich, F., and Gendron-Badou, A. (2002). "La Spectroscopie Infrarouge, Un Outil Polyvalent," in *Géologie de la Préhistoire : Méthodes, techniques et applications*. Editor J. C. Miskovsky (Paris: Géopré, Presses Universitaires de Perpignan), 663–677.

Goldberg, P., and Berna, F. (2010). Micromorphology and Context. *Quat. Int.* 214 (1-2), 56–62. doi:10.1016/j.quaint.2009.10.023

Guilloré, P. (1985). *Méthode de fabrication mécanique et en série de lames minces. Polycopié*. Paris-Grignon: Institut National Agronomique.

Hassan, F. A. (1978). Sediments in Archaeology: Methods and Implications for Palaeoenvironmental and Cultural Analysis. *J. Field Archaeol.* 5, 197–213. doi:10.1179/009346978791489899

Jaillard, B. (1992). Calcification des cellules corticales des racines en milieu calcaire. *Bull. la Société Bot. Fr. Actual. Bot.* 139 (1), 41–46. doi:10.1080/01811789.1992.10827086

Jaillard, B., and Callot, G. (1987). "Action des racines sur la ségrégation minéralogique des constituants du sol," in *Micromorphologie des Sols (Soil Micromorphology)*. Editors N. Fedoroff, L. M. Bresson, and M. A. Courty (Paris: AFES), 371–375.

Jaillard, B., Guyon, A., and Maurin, A. F. (1991). Structure and Composition of Calcified Roots, and Their Identification in Calcareous Soils. *Geoderma* 50, 197–210. doi:10.1016/0016-7061(91)90034-q

Jamagne, M., Jeanson, C., and Eimberck, M. (1987). "Données sur la composition des argilanes en régions tempérées et continentales," in *Micromorphologie des Sols (Soil Micromorphology)*. Editors N. Fedoroff, L. M. Bresson, and M. A. Courty (Paris: AFES), 279–289.

Jongmans, A. G., Pulleman, M. M., and Marinissen, J. C. Y. (2001). Soil Structure and Earthworm Activity in a Marine Silt Loam under Pasture versus Arable Land. *Biol. Fertil. Soils* 33, 279–285. doi:10.1007/s003740000318

Karkanas, P., Bar-Yosef, O., Goldberg, P., and Weiner, S. (2000). Diagenesis in Prehistoric Caves: The Use of Minerals that Form *In Situ* to Assess the Completeness of the Archaeological Record. *J. Archaeol. Sci.* 27, 915–929. doi:10.1006/jasc.1999.0506

Karkanas, P., and Goldberg, P. (2019). *Reconstructing Archaeological Sites. Understanding the Geoarchaeological Matrix"*. Chichester: John Wiley & Sons.

Karkanas, P. (2010). Preservation of Anthropogenic Materials under Different Geochemical Processes: A Mineralogical Approach. *Quat. Int.* 214 (1), 63–69. doi:10.1016/j.quaint.2009.10.017

Kühn, P., Aguilar, J., and Miedema, R. (2010). "Textural Pedofeatures and Related Horizons," in *Interpretation of Micromorphological Features of Soils and Regoliths*. Editors G. Stoops, V. Marcelino, and F. Mees (Amsterdam: Elsevier), 217–250.

Le Drészen, Y. (2008). *Dynamiques des paysages de la vallée du Yamé depuis 4000 ans. Contribution à la compréhension d'un géosystème soudano-sahélien. (Ounjougou, Pays dogon, Mali)*. Doctoral Thesis. Caen, France: Université de Caen.

Lucas, G., and Montenat, C. (1967). Observations sur les structures internes et le développement des Microcodiums. *Bull. Société géologique Française* 7 (9), 909–918. doi:10.2113/gssgfbull.s7-ix.6.909

Lyman, R. L. (1994). *Vertebrate Taphonomy*. Cambridge: Cambridge University Press.

Mallol, C., Mentzer, S. M., and Miller, C. E. (2017). "Combustion Features," in *Archaeological Soil and Sediment Micromorphology*. Editors C. Nicosia and G. Stoops (Chichester: John Wiley & Sons), 299–330. doi:10.1002/9781118941065.ch31

Mallol, C., VanNieuwenhuyse, D., and Zaidner, Y. (2011). Depositional and Paleoenvironmental Setting of the Bizat Ruhama Early Pleistocene Archaeological Assemblages, Northern Negev, Israel: A Microstratigraphic Perspective. *Geoarchaeology* 26, 118–141. doi:10.1002/gea.20339

Mallol, C. (2006). What's in a Beach? Soil Micromorphology of Sediments from the Lower Paleolithic Site of 'Ubeidiya, Israel. *J. Hum. Evol.* 51 (2), 185–206. doi:10.1016/j.jhevol.2006.03.002

Massenet, J. Y. (2008). "Typologie des sols," in *Le référentiel pédologique. Association Française pour l'Etude des Sols* (Versailles. Éditions Quæ.

Miskovsky, J. C., and Debard, E. (2002). "Granulométrie des sédiments et étude de leur fraction grossière," in *Géologie de la Préhistoire : Méthodes, techniques, applications*. Editor J. C. Miskovsky (Paris: Géopré, Presses Universitaires de Perpignan), 480–501.

Parés, J. M., Sahnouni, M., Van der Made, J., Pérez-González, A., Harichane, Z., Derradji, A., et al. (2014). Early Human Settlements in Northern Africa: Paleomagnetic Evidence from the Ain Hanech Formation (Northeastern Algeria). *Quat. Sci. Rev.* 99, 203–209. doi:10.1016/j.quascirev.2014.06.020

Picq, C., Laporte, L., Cammas, C., Marambat, L., Gruet, Y., and Genre, C. (2002). La dynamique de comblement du vallon et son paléoenvironnement. *galip* 44, 8–25. doi:10.3406/galip.2002.2053

Sahnouni, M., and de Heinzelin, J. (1998). The Site of Ain Hanech Revisited: New Investigations at This Lower Pleistocene Site in Northern Algeria. *J. Archaeol. Sci.* 25, 1083–1101. doi:10.1006/jasc.1998.0278

Sahnouni, M., Everet, M., Van der Made, J., and Harichane, Z. (2017). Mise en évidence d'un changement climatique dans le site pléistocène inférieur d'El Kherba (Algérie), et son possible impact sur les activités des hominidés, il y a 1,7 Ma. *L'Anthropologie* 121, 146–162. doi:10.1016/j.anthro.2017.03.015

Sahnouni, M., Hadjouis, D., Van der Made, J., Derradji, A., Canals, A., Medig, M., et al. (2002). Further Research at the Oldowan Site of Ain Hanech, North-eastern Algeria. *J. Hum. Evol.* 43, 925–937. doi:10.1006/jhev.2002.0608

Sahnouni, M. J., and Van der Made, J. (2009). "The Oldowan in North Africa within a Biochronological Framework," in *The Cutting Edge: New Approaches to the Archaeology of Human Origins*. Editors N. Toth and K. Schick (Bloomington: Stone Age Institute Press), 179–210.

Sahnouni, M., Parés, J. M., Duval, M., Cáceres, I., Harichane, Z., Van der Made, J., et al. (2018). 1.9-million- and 2.4-Million-Year-Old Artifacts and Stone Tool–Cutmarked Bones from Ain Boucherit, Algeria. Science, 362 (6420), 1297130. doi:10.1126/science.Aau0008

Sahnouni, M., Rosell, J., Van der Made, J., Vergès, J. M., Ollé, A., Kandi, N., et al. (2013). The First Evidence of Cut Marks and Usewear Traces from the Plio-Pleistocene Locality of El-Kherba (Ain Hanech), Algeria: Implications for Early Hominin Subsistence Activities Circa 1.8 Ma. *J. Hum. Evol.* 64, 137–150. doi:10.1016/j.jhevol.2012.10.007

Sahnouni, M. (1998). "The Lower Palaeolithic of the Maghreb: Excavations and Analyses at Ain Hanech, Algeria," in *Cambridge Monograph in African Archaeology, British Archaeological Report International Series* (Oxford: Archaeopress), 689. doi:10.30861/9780860548751

Sahnouni, M. (2006). "The North African Early Stone Age and the Sites at Ain Hanech, Algeria," in *The Oldowan: Case Studies into the Earliest Stone Age*. Editors N. Toth and K. Schick (Bloomington: Stone Age Institute Press), 77–111.

Sahnouni, M., Van der Made, J., and Everett, M. (2011). Ecological Background to Plio-Pleistocene Hominin Occupation in North Africa: the Vertebrate Faunas from Ain Boucherit, Ain Hanech and El-Kherba, and Paleosol Stable-Carbon-Isotope Studies from El-Kherba, Algeria. *Quat. Sci. Rev.* 30, 1303–1317. doi:10.1016/j.quascirev.2010.01.002

Schick, K. D. (1986). *Stone Age Sites in the Making*, 319. Oxford: British Archaeological Reports International Series.

Shahack-Gross, R., Berna, F., Karkanas, P., and Weiner, S. (2004). Bat Guano and Preservation of Archaeological Remains in Cave Sites. *J. Archaeol. Sci.* 31, 1259–1272. doi:10.1016/j.jas.2004.02.004

Shipman, P. (1981). *Life History of a Fossil: An Introduction to Taphonomy and Paleoecology*. Cambridge: Harvard University Press.

Stephan, E. (2000). Oxygen Isotope Analysis of Animal Bone Phosphate: Method Refinement, Influence of Consolidants, and Reconstruction of Palaeotemperatures for Holocene Sites. *J. Archaeol. Sci.* 27, 523–535. doi:10.1006/jasc.1999.0480

Vallverdú, J., Courty, M. A., Carbonell, E., Canals, A., and Burjachs, F. (2001). Les sédiments d'*Homo Antecessor* de Gran Dolina, (Sierra de Atapuerca, Burgos, Espagne). *Interprétation Micromorphol. des Process. de Form. enregistrement paléoenvironnemental des sédiments. L'Anthropologie* 105, 45–69. doi:10.1016/s0003-5521(01)80005-4

Conflict of Interest: The authors declare that the research was conducted in the absence of any commercial or financial relationships that could be construed as a potential conflict of interest.

Publisher's Note: All claims expressed in this article are solely those of the authors and do not necessarily represent those of their affiliated organizations, or those of the publisher, the editors, and the reviewers. Any product that may be evaluated in this article, or claim that may be made by its manufacturer, is not guaranteed or endorsed by the publisher.